SOME PROMISING LINES OF DEVELOPMENT FOR FUTURE COMPUTER APPLICATIONS IN MULTI-REACH CANALS AND BRANCHING SYSTEMS

D.L. Fread*

April 9,1985

INTRODUCTION

Unsteady flow simulation (channel routing) models mathematically predict the changing magnitude, speed, and shape of a water wave as it propagates through canals, rivers, reservoirs, or estuaries. The water wave can emanate from precipitation runoff (rainfall or snow-melt), reservoir releases (spillway flows or dam-failures), and tides (astronomical and/or wind-generated).

Channel routing has long been of vital concern to man as he has sought to predict the characteristic features of a water wave in his efforts to improve the transport of water through man-made or natural channels and to determine necessary actions to protect life and property from the effects of flooding. Commencing with investigations as early as the 17th century, mathematical techniques to predict wave propagation have continually been developed. With the contribution of Saint-Venant (1871), the basic theory for one-dimensional analysis of water wave propagation was formulated; however, due to the mathematical complexity of Saint-Venant's theoretical equations, simplifications were necessary to obtain feasible solutions for the salient characteristics of the wave. Thereafter, a profusion of simplified routing methods appeared in the literature. It is only within the last 25 years, with the advent of high-speed electronic computers, that the complete Saint-Venant equations could be solved with varying degrees of feasibility.

This paper describes the mathematical formulation and capabilities of a one-dimensional unsteady flow model, "FLDWAV", which is an enhancement of another model "DWOPER" (Fread, 1978). The latter has been used by the National Weather Service, Corps of Engineers, and many other governmental agencies, and private consulting firms, both nationally and internationally. Although FLDWAV and DWOPER have had limited application to irrigation systems, FLDWAV has the potential for simulating complex unsteady flow phenomena in simple or complex networks of irrigation channels having time-dependent flow and level controls. The FLDWAV Model can provide the necessary information on flow rates and water levels throughout the irrigation system for either real-time simulation and decision making or operational planning and design. The model could also be used to study unusual occurrences such as levee overtopping and/or failure as well as landslide blockages. It requires the computational resources of a mainframe or minicomputer for best performance although it can be used on microcomputers.

*Senior Research Hydrologist, Hydrologic Research Laboratory, National Weather Service, NOAA, 8060 13th Street, Silver Spring, Maryland 20910

The following special features are included in FLDWAV: variable Δt and Δx computational intervals; irregular cross-sectional geometry; off-channel storage; roughness coefficients which vary with discharge or water surface elevation, and distance along the channel; capability to generate linearly interpolated cross sections and roughness coefficients between input cross sections; automatic computation of initial steady flow and water elevations at all cross sections along the channel; external boundaries of discharge or water surface elevation time series (hydrographs), a single-valued or looped depth-discharge relation (tabular or computed); time dependent lateral inflows (outflows); internal boundaries which enable the treatment of time dependent reservoir spillway flows, gate controls; levee failure and/or overtopping; a special computational technique to provide numerical stability when treating flows which change from supercritical to subcritical or, conversely, with time and distance along the channel; and an automatic calibration technique for determining the variable roughness coefficient by using observed hydrographs along the channel.

FLDWAV is coded in FORTRAN IV and the computer program is of modular design with an overall program storage requirement of approximately 256000 bytes. Program array sizes are variable with the size of each array set internally via the input parameters used to describe the particular unsteady flow application for which the model is being used. Program output is user selective and consists of tabular and/or graphical displays.

BASIC ALGORITHM

FLDWAV is based on an implicit finite difference solution of the conservation form of the Saint-Venant equations of unsteady flow. In their conservation form, the equations consist of the conservation of mass equation, i.e.,

$$\frac{\partial Q}{\partial x} + \frac{\partial (A + A_o)}{\partial t} - q = 0 \tag{1}$$

and the conservation of momentum equation, i.e.,

$$\frac{\partial Q}{\partial t} + \frac{\partial (Q^2/A)}{\partial x} + gA \left(\frac{\partial h}{\partial x} + S_f + S_e\right) + L + W_f B = 0 \tag{2}$$

where:

$$S_f = \frac{n^2 |Q| Q}{2.21 A^2 R^{4/3}} \tag{3}$$

$$S_e = \frac{K_e \partial (Q/A)^2}{2g \partial x} \tag{4}$$

$$W_f = C_w (V_r \cos \omega)^2 \tag{5}$$

in which x is distance along the longitudinal axis of the channel, t is time, Q is discharge, A is active cross-sectional area, A_o is inactive (off-channel storage) cross-sectional area, q is lateral inflow (positive) or outflow

(negative), g is the gravity acceleration constant, h is water surface elevation, B is wetted top width of cross section, L is the momentum effect of lateral inflow, S_f is friction slope computed from Manning's equation, n is the Manning n, R is the hydraulic radius, S_e is the local loss slope, K_e is an expansion (negative) or contraction (positive) coefficient, W_f is the wind term, C_w is non-dimensional wind coefficient, V_r is the velocity of the wind (V_w, + if opposing flow and - if aiding the flow) relative to the velocity of the channel flow, and ω is the angle between the wind direction and channel flow direction.

In an implicit finite difference solution of Eqs. (1) and (2), the continuous x-t solution domain in which solutions of h and Q are sought is represented by a rectangular net of discrete points as shown in Fig. 1. The net points (nodes) may be at equal or unequal intervals of Δt and Δx along the t and x axes, respectively. Each node is identified by a subscript (i) which designates the x position and a superscript (j) for the time line. A four-point weighted, implicit difference approximation is used to transform the

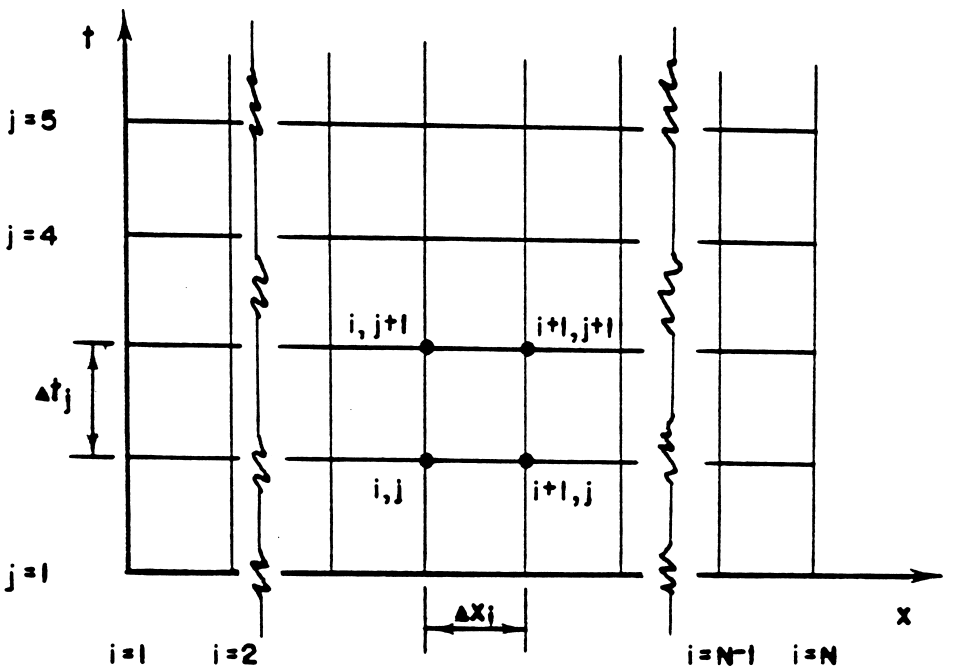

Figure 1. The x-t Solution Region.

nonlinear partial differential equations of Saint-Venant into nonlinear algebraic equations. The four-point weighted difference approximations similar to that used by Preissmann (1961) are:

$$\frac{\partial K}{\partial t} = \left(K_i^{j+1} + K_{i+1}^{j+1} - K_i^j - K_{i+1}^j\right)/(2\Delta t^j) \tag{6}$$

$$\frac{\partial K}{\partial x} = \theta/\Delta x_i \left(K_{i+1}^{j+1} - K_i^{j+1}\right) + (1-\theta)/\Delta x_i \left(K_{i+1}^j - K_i^j\right) \tag{7}$$

$$K = 0.5\ \theta \left(K_i^{j+1} + K_{i+1}^{j+1}\right) + 0.5(1-\theta) \left(K_i^j + K_{i+1}^j\right) \tag{8}$$

where K is a dummy parameter representing any variable in the above differential equations, θ is a weighting factor varying from 0.5 to 1, i is a subscript denoting the sequence number of the cross section or Δx reach, and j is a superscript denoting the sequence number of the time line in the x-t solution domain. A θ value of 0.5 is known as the "box" scheme while $\theta = 1$ is the "fully implicit" scheme. To insure unconditional linear numerical stability and provide good accuracy, θ values nearer to 0.5 are recommended (Fread, 1974). Accuracy decreases as θ departs from 0.5 and approaches 1.0. This effect becomes more pronounced as the time step size increases. FLDWAV allows θ to be an input parameter. A value of 0.55 to 0.60 is often used to minimize loss of accuracy while avoiding weak or pseudo instability which sometimes results when θ of 0.5 is used.

Substitution of the finite difference approximations defined by Eqs. (6)-(8) into Eqs. (1) and (2) for the derivatives and non-derivative terms and multiplying through by Δx_i yields the following difference equations:

$$\begin{aligned}
&\theta \left(Q_{i+1}^{j+1} - Q_i^{j+1} - \bar{q}_i^{j+1}\ \Delta x_i\right) + (1-\theta) \left(Q_{i+1}^j - Q_i^j - \bar{q}_i^j\ \Delta x_i\right) \\
&+ 0.5\ \Delta x_i/\Delta t^j \left[(A + A_o)_i^{j+1} + (A + A_o)_{i+1}^{j+1} - (A + A_o)_i^j\right. \\
&\left. - (A + A_o)_{i+1}^j\right] = 0
\end{aligned} \tag{9}$$

$$\begin{aligned}
&0.5\ \Delta x_i/\Delta t^j \left(Q_{i+1}^{j+1} + Q_i^{j+1} - Q_i^j - Q_{i+1}^j\right) + \theta\left[(Q^2/A)_{i+1}^{j+1}\right. \\
&- (Q^2/A)_i^{j+1} + g\ \bar{A}_i^{j+1} \left(h_{i+1}^{j+1} - h_i^{j+1} + \Delta x_i\ \bar{S}_{f_i}^{j+1} + \Delta x_i\ \bar{S}_{e_i}^{j+1}\right) \\
&\left. + \Delta x_i \left(L + \bar{W}_f \bar{B}\right)_i^{j+1}\right] + (1-\theta) \left[(Q^2/A)_{i+1}^j - (Q^2/A)_i^j + g\bar{A}_i^j\right. \\
&\left. \left(h_{i+1}^j - h_i^j + \Delta x_i\ \bar{S}_{f_i}^j + \Delta x_i\ \bar{S}_{e_i}^j\right) + \Delta x_i \left(L + \bar{W}_f \bar{B}\right)_i^j\right] = 0
\end{aligned} \tag{10}$$

where: $\bar{A}_i = 0.5\ (A_i + A_{i+1})$ (11)

$\bar{B}_i = 0.5\ (B_i + B_{i+1})$ (12)

$$\bar{S}_{f_i} = \frac{\bar{n}_i^{\,2} |\bar{Q}_i| \bar{Q}_i}{2.21\ \bar{A}_i^{\,2}\ R_i^{\,4/3}} \quad (13)$$

$\bar{Q}_i = 0.5\ (Q_i + Q_{i+1})$ (14)

$R_i = \bar{A}_i / \bar{B}_i$ (15)

or $R_i = \bar{A}_i / \bar{P}_i$ (16)

$\bar{S}_{e_i} = K_{e_i} \left[(Q/A)^2_{i+1} - (Q/A)^2_i \right] / (2g\,\Delta x_i)$ (17)

$\bar{W}_{f_i} = C_{w_i} |\bar{V}_{r_i}| \bar{V}_{r_i}$ (18)

$\bar{V}_{r_i} = \bar{Q}_i / \bar{A}_i - \bar{V}_{w_i} \cos\ \omega$ (19)

$L_i = - (\overline{qv_x})_i$ (lateral inflow) (20)

$L_i = - (\bar{q}\ \bar{Q}/\bar{A})_i$ (bulk lateral outflow) (21)

$L_i = - (0.5\ \bar{q}\ \bar{Q}/\bar{A})_i$ (seepage lateral outflow) (22)

The bar (-) above the variables represents the average of the variable over the reach length (Δx_i) between cross sections i and i+1. The subscript (i) associated with $\bar{q}$, $\bar{v}_x$, $\bar{A}$, $\bar{B}$, $\bar{S}_f$, $\bar{Q}$, $\bar{S}_e$, $\bar{W}_f$, $\bar{V}_r$, and $\bar{V}_w$ represents the number of the reach (Δx_i) rather than the cross section (node) number. Node numbers commence with 1 and terminate with N, while reach numbers commence with 1 and terminate with (N-1).

Eqs. (9) and (10) are nonlinear with respect to the unknowns h and Q at the points i and i+1 on the j+1 time line. All terms associated with the j^{th} time line are known from either the initial conditions or previous computations. The initial conditions are values of h and Q at each computational point (node) along the x-axis for the first time line (j=1).

Eqs. (9) and (10) are two nonlinear algebraic equations which cannot be solved in a direct (explicit) manner since there are four unknowns, h and Q, at points i and (i+1) on the (j+1) time line and only two equations. However, if similar equations are formed for each of the (N-1) Δx reaches between the upstream and downstream boundaries, a total of (2N-2) equations with 2N unknowns results. (N denotes the total number of computational points or cross sections.) Then prescribed boundary conditions, one at the upstream extremity of the channel and one at the downstream extremity, provide the additional two equations required for the system to be determinate. The resulting system of 2N nonlinear equations with 2N unknowns is solved by the Newton-Raphson method which was first applied by Amein and Fang (1970) to an implicit nonlinear formulation of the Saint-Venant equations.

Newton-Raphson Method. The Newton-Raphson method is a functional iterative technique to solve a system of nonlinear equations. The technique is derived from a Taylor series expansion of the nonlinear function in which all terms of second and higher order are neglected. The resulting algorithm is:

$$J'(X^k)\ \Delta X = -\ f(X^k) \tag{23}$$

in which X^k is a vector quantity, J' is the Jacobian (a coefficient matrix made up of the partial derivatives evaluated with X^k values), $f(X^k)$ is the nonlinear equation evaluated with X^k values, and ΔX is a vector containing the 2N unknowns. Eq. (23) represents a system of equations in which the unknown vector ΔX is linear. Solution of Eq. (23) for the unknown ΔX by an appropriate matrix inversion technique such as Gauss elimination. The ΔX vector actually represents the difference between an initial estimate of the true solution and an improved estimate, i.e.,

$$\Delta X = X^{k+1} - X^k \tag{24}$$

in which k is the number of iteration, X^k is the initial estimate (guess) and X^{k+1} is the improved estimate. Convergence of the iterative solution is attained in usually one or two iterations when the ΔX vector containing the unknown discharges $(Q_i^{j+1}, Q_{i+1}^{j+1})$ and water elevations $(h_i^{j+1}, h_{i+1}^{j+1})$ becomes less than convergence criteria which are specified for each application of FLDWAV. Typical values are 0.01 ft. for convergence of water elevation (ε_h)while the convergence for the discharge is specified in ft^3/sec according to the following relation:

$$\varepsilon_Q = \varepsilon_h \hat{B} \hat{V} \tag{25}$$

in which $\hat{B}$ and $\hat{V}$ are the representative channel width and velocity, respectively.

The convergence process depends on a good first estimate for the vector X^k. A reasonably accurate initial condition of the discharges and water

elevations at t = 0 provides the first X^k. Thereafter, X^k first estimate values can be obtained using extrapolated values from solutions at previous time steps according to the following algorithm:

$$X^k = X^{j-1} + (X^{j-1} - X^{j-2})\ \alpha'\ \Delta t^j / \Delta t^{j-1} \tag{26}$$

where Δt^j and Δt^{j-1} are values of time steps between the time lines corresponding to the solution vectors, X^j and X^{j-1}, respectively. The weighting factor α' can be specified over the range of zero to unity.

The Jacobian matrix, $J'(X^k)$, is composed of elements ($a_{\ell,k}$) located along the main-diagonal with two elements in rows 1 and 2N which represent the upstream and downstream external boundaries, respectively; and all other rows have four elements which represent the partial derivatives of Eqs. (9) and (10) with respect to the four unknowns (Q_i^{j+1}, h_i^{j+1}, Q_{i+1}^{j+1}, h_{i+1}^{j+1}). Each adjacent pair of rows represent the application of Eqs. (9) and (10) to each Δx_i reach along the channel proceeding from the upstream to the downstream boundary.

Thus, the Newton-Raphson method generates a system of 2N x 2N linear equations. The Jacobian or coefficient matrix of the system is composed of the partial derivative expressions evaluated at the first estimate, X^k. The right-hand side of Eq. (23) is the residual, a vector whose values are obtained by evaluating Eqs. (9) and (10) using the X^k estimate values for the unknown discharges and water surface elevations. Solution of the linear system described by Eq. (23) provides corrections to the first trial (estimated) values of the unknowns.

Matrix Solution. An efficient matrix solution technique is critical to the feasibility of an implicit model. Eq. (23) is solved by a special modification of the Gauss elimination method for solving a system of linear equations. Using matrix notation, Eq. (23) takes the following form:

$$[A]\ X = R \tag{27}$$

in which [A] = the coefficient matrix with elements $a_{\ell,k}$ and X, R are column vectors having components x_ℓ and r_ℓ respectively. The coefficient matrix is banded with most of the elements being zero except for four elements in each row along the main-diagonal of the matrix. An efficient solution technique was developed by Fread (1971) in which (1) the computations do not involve any of the many zero elements, thus reducing the required number of operations (addition, subtraction, division, multiplication) from ($16/3N^3 + 8N^2 + 14/3N$) to ($38N - 19$); and (2) stores only the non-zero elements, thus reducing the storage required for the [A] matrix from 2N x 2N to 2N x 4, where N is the total number of cross sections along the channel. The compaction of the original matrix into 2N x 4 size causes the subscript k in Eqs. (14-87) -

(14-94) not to increment for each successive Δx reach, i.e., k=1,2,3,4, for all ℓ rows.

Eq. (27) may be efficiently solved by the following compact, penta-diagonal, modified Gauss elimination algorithm. The computations to eliminate the elements below the main-diagonal proceed according to $\ell = 2,4,6 \ldots 2N-2$ and are:

$$a_{\ell,2} = -a_{\ell,1}/a_{\ell-1,k'+1}\ a_{l-1,k'+2} + a_{\ell,2} \tag{28}$$

$$r_{\ell} = -a_{\ell,1}/a_{\ell-1,k'+1}\ r_{\ell-1} + r_{\ell} \tag{29}$$

$$a_{\ell+1,2} = -a_{\ell+1,1}/a_{\ell-1,k'+1}\ a_{\ell-1,k'+2} + a_{\ell+1,2} \tag{30}$$

$$r_{\ell+1} = -a_{\ell+1,1}/a_{\ell-1,k'+1}\ r_{\ell-1} + r_{\ell+1} \tag{31}$$

$$a_{\ell+1,3} = -a_{\ell+1,2}/a_{\ell,2}\ a_{\ell,3} + a_{\ell+1,3} \tag{32}$$

$$a_{\ell+1,4} = -a_{\ell+1,2}/a_{\ell,2}\ a_{\ell,4} + a_{\ell+1,4} \tag{33}$$

$$r_{\ell+1} = -a_{\ell+1,2}/a_{\ell,2}\ r_{\ell} + r_{\ell+1} \tag{34}$$

in which k' = 0 when $\ell = 2$ and k' =2 when $\ell > 2$. The x_{ℓ} components of the solution vector X are obtained through a back-substitution procedure commencing at $\ell = 2N$ and proceeding sequentially to $\ell = 1$. Thus,

$$x_{2N} = (-a_{2N,3}/a_{2N-1,3}\ r_{2N-1} + r_{2N})/ (-a_{2N,3}/a_{2N-1,3}\ a_{2N-1,4} + a_{2N,4}) \tag{35}$$

$$x_{\ell} = (r_{\ell} - a_{\ell,k'+2}\ x_{\ell+1})/a_{\ell,k'+1} \quad \ldots \ell = 2N-1,2N-3,\ldots 3,1 \tag{36}$$

$$x_{\ell} = (r_{\ell} - a_{\ell,4}\ x_{\ell+2} - a_{\ell,3}\ x_{\ell+1})/a_{\ell,2} \quad \ldots \ell = 2N-2,2N-4,\ldots 4,2 \tag{37}$$

in which k' = 2 when $\ell > 1$ and k' = 0 when $\ell = 1$.

Enhancement of Computational Algorithm. FLDWAV contains an automatic procedure which increases the robust nature of the four-point, nonlinear implicit finite difference algorithm. This enhancement is quite useful when treating rapidly rising hydrographs in channels where the cross sections have large variations in the vertical and/or along the x-axis. This situation may cause computational problems which are manifested by non-convergence in the

Newton-Raphson iteration or by erroneously low computed depths at the leading edge of steep-fronted waves. When either of these manifestations are sensed, an automatic procedure consisting of two parts is implemented.

The first reduces the current time step (Δt) by a factor of 1/2 and repeats the computations. If the same problem persists, Δt is again halved and the computations repeated. This continues until a successful solution is obtained or the time step has been reduced to 1/16 of the original size. If a successful solution is obtained, the computational process proceeds to the next time level using the original Δt. If the solution using $\Delta t/16$ is unsuccessful, the θ weighting factor is increased by 0.1 and a time step of $\Delta t/2$ is used. Upon achieving a successful solution, θ and the time step are restored to their original values. Unsuccessful solutions are treated by increasing θ and repeating the computation until $\theta = 1.0$ whereupon the automatic procedure terminates and the solution with $\theta = 1.$ and $\Delta t/2$ is used to advance the solution forward in time now using the original θ and Δt values. Often, computational problems can be overcome via one or two reductions in the time step.

EXTERNAL BOUNDARIES AND INITIAL CONDITIONS

External boundaries which consist of the upstream and downstream extremities of the channel must be specified in order to obtain solutions to the Saint-Venant equations. In fact, in most unsteady flow applications, the unsteady disturbance is introduced to the channel at one or both of the external boundaries.

Upstream Boundary. Either a specified discharge or water elevation time series (hydrographs) can be used as the upstream boundary in FLDWAV. If a discharge hydrograph Q(t) is used, the boundary equation is:

$$\hat{B}_1 = Q_1^{j+1} - Q(t) = 0 \qquad (38$$

If a water elevation time series h(t) is used, the boundary equation is:

$$\hat{B}_1 = h_1^{j+1} - h(t) = 0 \qquad (39$$

The hydrographs used as upstream boundary conditions should not be affected by the flow conditions downstream of the upstream boundary.

Downstream Boundary. Specified discharge or water elevation time series may be used as the downstream boundary condition. For a discharge hydrograph Q'(t), the boundary equation is:

$$\hat{B}_N = Q_N^{j+1} - Q'(t) = 0 \qquad (40$$

If a water elevation time series h'(t) such as an observed or predicted tide or lake level, the boundary equation is:

$$\hat{B}_N = h_N^{j+1} - h'(t) = 0 \qquad (41$$

Another frequently used downstream boundary is a relation between discharge and depth or water elevation such as a single-valued rating curve expressed in tabular (piece-wise linear) form consisting of points (Q_k, h_k)

Any discharge Q' can be obtained from the table for any associated water elevation (h_N^{j+1}) at the downstream boundary by the following linear interpolation formula:

$$Q' = Q_k + (Q_{k+1} - Q_k)\ (h_N^{j+1} - h_k)/(h_{k+1} - h_k) \tag{42}$$

In this case, the downstream boundary equation is:

$$\hat{B}_N = Q_N^{j+1} - Q' = 0 \tag{43}$$

The downstream boundary can be a loop-rating curve based on the Manning equation for normal flow. The loop is produced by using the water surface slope rather than the channel bottom slope. In this case, the downstream boundary equation is:

$$\hat{B}_N = Q_N^{j+1} - QN = 0 \tag{44}$$

where:
$$QN = 1.49 \left(\frac{A^{5/3}}{nB^{2/3}}\right)_N^{j+1} \left(\frac{h_{N-1}^j - h_N^j}{\Delta x_{N-1}}\right)^{1/2} \tag{45}$$

The downstream boundary can be a critical flow section; the downstream boundary equation is:

$$\hat{B}_N = Q_N^{j+1} - QC = 0 \tag{46}$$

where:
$$QC = \left(\sqrt{g/B}\ A^{3/2}\right)_N^{j+1} \tag{47}$$

The flow at the downstream boundary should not be affected by flow conditions further downstream. Of course, there are always some minor influences on the flow due to the presence of cross-sectional irregularities downstream of the chosen boundary location; however, these usually can be neglected unless the irregularity is very pronounced such as to cause significant backwater or drawdown effects. Reservoirs or major tributaries located below the downstream boundary which cause backwater effects at the chosen boundary location should be avoided. When this situation is unavoidable, the reach of channel for which the Saint-Venant equations are being used should be extended on downstream to a location below where the tributary enters or to the dam in the case of the reservoir. Sometimes the routing reach may be shortened and the downstream boundary shifted upstream to a point where backwater effects are negligible.

Initial Conditions. Initial conditions of water surface elevation (h) and discharge (Q) must be specified at time t = 0 to obtain solutions of the Saint-Venant equations. Initial conditions may be specified for FLDWAV by any of the following: (1) from observations at gaging stations with interpolated values for intermediate cross sections; these must be sufficiently accurate to result in convergence of the Newton-Raphson solution of the Saint-Venant finite difference equations (the errors dampen-out after several time steps);

(2) computed values from a previous unsteady flow solution (this is frequently used in day-to-day flood forecasting); and 3) computed values from a steady flow backwater solution.

In the case of steady flow, the discharge at all cross sections can be determined by:

$$Q_{i+1} = Q_i + \bar{q}_i \, \Delta x_i \qquad \ldots \; i = 1,2,3, \ldots N-1 \qquad (48)$$

in which Q_1 is the assumed steady flow at the upstream boundary at time t=0, and $\bar{q}_i$ is the known average lateral inflow (outflow) along each Δx reach at t=0. The water surface elevations (h_i) are computed according to the following steady flow simplification of the momentum Eq. (14-62):

$$(Q^2/A)_{i+1} - (Q^2/A)_i + g\bar{A}_i \, (h_{i+1} - h_i + \Delta x_i \, \bar{S}_{f_i}) = 0 \qquad (49)$$

in which $\bar{A}_i$ and $\bar{S}_{f_i}$ are defined by Eqs. (11) and (13), respectively. The computations proceed in the upstream direction (i = N-1, ... 3,2,1) for subcritical flow (they proceed in the downstream direction for supercritical flow). The starting water surface elevation (h_N) can be specified or obtained from the appropriate downstream boundary condition for a discharge of Q_N. Eq. (49) can be solved by the Newton-Raphson method as applied to a single nonlinear equation. In this case, if Eqs. (23) and (24) are combined, the following recursive relationship can be written in scalar form:

$$x^{k+1} = x^k - f(x^k)/f'(x^k) \qquad (50)$$

in which x represents the unknown (h_i), k is the number of iterations, $f(x^k)$ is Eq. (49) evaluated with the trial solution x^k, and $f'(x^k)$ is the derivative of Eq. (49) with respect to the unknown (h_i) and evaluated at x^k.

INTERNAL BOUNDARIES

There may be locations along the channel(s) at which structures control the flow or level such as a dam, bridge, or waterfall (short rapids) where the Saint-Venant equations are not applicable. At these locations, the flow is often rapidly varied rather than gradually varied as necessary for the applicability of the Saint-Venant equations. Empirical water elevation-discharge relations such as weir-flow can be utilized for simulating rapidly varying flow. In FLDWAV, unsteady flows are routed along the channel including points of rapidly varying flow by utilizing internal boundaries. At internal boundaries, cross sections are specified for the upstream and downstream extremities of the section of channel where rapidly varying flow occurs. The Δx reach length between the two cross sections can be any appropriate value from zero to the actual measured distance. Since, as with any other Δx reach, two equations (the Saint-Venant equations) are required, the internal boundary Δx reach requires two equations. The second of the required equations represents the conservation of mass with negligible time-dependent storage, i.e.,

$$\hat{B}_{I2} = Q_i^{j+1} - Q_{i+1}^{j+1} = 0 \tag{51}$$

The first of the two required equations is an empirical rapidly varied flow relation. Several examples of rapidly varied flow internal boundary equations follow.

Critical Flow. If the internal boundary is used to represent critical flow, the following equation is used in conjunction with Eq. (51):

$$\hat{B}_{I1} = Q_i^{j+1} - \sqrt{g}\,(A^{3/2}/B^{1/2})_i^{j+1} = 0 \tag{52}$$

Rating Curve. A rating curve as described previously in the section, "External Boundaries and Initial Conditions", can be used as an internal boundary in which the downstream flow is assumed to have negligible effect on the flow passing the internal boundary section. The internal boundary equation is:

$$\hat{B}_{I1} = Q_i^{j+1} - Q' = 0 \tag{53}$$

in which Q' is defined by Eq. (42).

Dam. At a dam, the internal boundary can represent any combination of flow such as spillway flow (uncontrolled overflow, fixed gate, time-dependent gate), crest overflow, constant (head-independent) flow, or breach flow due to a time-dependent failure of the dam. The general equation for flow at a dam is:

$$\hat{B}_{I1} = Q_i^{j+1} - Q_s = 0 \tag{54}$$

in which Q_s is the spillway flow defined as follows:

$$Q_s = K_{ss}\,Q_{ss} + Q_g + K_{cs}\,Q_{cs} + Q_t \tag{55}$$

$$Q_{ss} = c_s\,L_s\,(h_i^{j+1} - h_s)^{3/2} \tag{56}$$

$$Q_g = \sqrt{2g}\,c_g\,A_g\,(h_i^{j+1} - h_g)^{1/2} \tag{57}$$

$$Q_{cs} = c_d\,L_d\,(h_i^{j+1} - h_d)^{3/2} \tag{58}$$

$$K_{ss} = 1. - 27.8\,(h_{rs} - 0.67)^3 \qquad \ldots\ h_{rs} > 0.67 \tag{59}$$

$$h_{rs} = (h_{i+1}^{j+1} - h_s)/(h_i^{j+1} - h_s) \tag{60}$$

$$K_{cs} = 1. - 27.8\ (h_{rc} - 0.67)^3 \qquad \ldots\ h_{rc} > 0.67 \tag{61}$$

$$h_{rc} = (h_{i+1}^{j+1} - h_d)/(h_i^{j+1} - h_d) \tag{62}$$

in which K_{ss} and K_{cs} are submergence correction factors for the spillway and dam crest, respectively; c_s, c_g, and c_d are discharge coefficients for the spillway, gate(s) and dam crest, respectively; L_s is the length of the spillway; A_g is the area of the gate opening; L_d is the length of the dam crest after subtracting L_s; h_s is the elevation of the spillway crest; h_g is the elevation of the center of the gate(s); and Q_t is a constant, head-independent outflow. Also, time-dependent gate parameters (c_g and A_g) may be specified via tabular, piece-wise linear, values and associated times (t).

Water Level Control. A channel may have a device which either manually or automatically causes the level immediately upstream to continually remain at the target elevation for a large range of flows. Although the actual changes in the level controller are not known, the maintenance of a constant water elevation provides the internal boundary equation, i.e.,

$$\hat{B}_{I1} = h_i^{j+1} - h_t = 0 \tag{63}$$

in which h_t is the target pool elevation upstream of the level control device.

Gated Flow Control. Several locations along a channel may have movable sluice gates whose settings are time-dependent to provide pre-determined flow rates to exist at such locations. An expression for the flow rate is used an internal boundary, i.e.,

$$\hat{B}_{I1} = Q_i^{j+1} - c_g A_g^{j+1} \sqrt{2g} (h_i^{j+1} - h_d)^{1/2} = 0 \tag{64}$$

where h_d is the gate sill elevation if the flow is unaffected by the downstream water elevation such as gate structures where the downstream channel bottom abruptly drops down. If the channel bottom is more or less continuous through the gate, h_d is downstream water elevation, i.e.,

$$h_d = h_{i+1}^{j+1} \ . \tag{65}$$

SUPERCRITICAL OR MIXED FLOW

In the preceding presentation, it was assumed the flow is always subcritical at each cross section along the routing reach. When the flow becomes supercritical, it requires special treatment of the external boundaries. Supercritical flow may occur all along a channel reach, or it may occur at intermittent locations along the routing reach. The former is easier to treat, while the latter ("mixed flow") is more difficult. The flow may be mixed in both time and location along the channel. The locations of each type of flow (supercritical or subcritical) must be determined at each time step, and various types of boundary conditions must be used with each partial reach of supercritical or subcritical flow.

Supercritical flow occurs when the Froude number (F_i) is greater than that for critical flow, i.e.,

$$F_i = Q_i / \left(\sqrt{g/B_i}\, A_i^{3/2} \right) > F_c \qquad (66)$$

in which F_c is the Froude number for critical flow. A value of 1.0 is used for F_c, although this may be slightly changed to account for numerical effects. Subcritical flow occurs when $F_i < F_c$, and critical flow occurs when $F_i = F_c$. A priori estimation of the occurrence of supercritical flow is conveniently determined through use of the channel bottom slope, i.e., supercritical flow occurs if $S_o > S_c$, where S_c (the critical slope) may be expressed as follows:

$$S_c = gn^2 / \left[2.21\ (A/B)^{1/3} \right] \qquad (67)$$

Supercritical Flow. If the entire routing reach is supercritical flow, the downstream boundary condition is no longer required since flow disturbances cannot propagate upstream; hence, the downstream boundary is superfluous. However, in order to have a determinate system of implicit difference equations, there must be 2N equations to match the 2N unknowns. The additional equation needed to make a determinate system is an additional upstream boundary equation in the form of a depth-discharge relation, i.e.,

$$\hat{B}_2 = Q_1^{j+1} - QS = 0 \qquad (68)$$

where:

$$QS = \left(\frac{1.486\ A^{5/3}}{n\ B^{2/3}} \right)_1^{j+1} \left(\frac{h_1^j - h_2^j}{\Delta x_1} \right)^{1/2} \qquad (69)$$

Mixed Flow. When the flow changes with either time or distance along the routing reach from supercritical to subcritical or, conversely, the flow is described as "mixed". During each time step, subreaches are delineated where supercritical or subcritical flow exists by computing the Froude number at each cross section and grouping consecutive Δx_i reaches into either subcritical or supercritical subreaches. Then, the Saint-Venant equations are applied and solutions obtained for each subreach, commencing with the most upstream subreach and progressing downstream until each subreach has been solved. Appropriate external boundary equations are used for each subreach.

Where the flow changes from subcritical to supercritical, the downstream boundary for the subcritical subreach is the critical flow Eq. (46). The two upstream boundary equations for the supercritical subreach are:

$$\hat{B}_{I1} = Q_1^{j+1} - Q' = 0 \tag{70}$$

$$\hat{B}_{I2} = h_1^{j+1} - h_c = 0 \tag{71}$$

in which Q' is the computed flow at the downstream boundary of subcritical subreach, Q_1^{j+1} is the flow at the same cross section which is now the first section of the supercritical subreach, h_c is the critical water surface elevation computed at the downstream boundary of the subcritical subreach, and h_1^{j+1} is the water elevation of the first section of the supercritical subreach. The supercritical subreach does not require a downstream boundary equation.

Where the flow changes from supercritical to subcritical, the upstream boundary equation for the subcritical subreach is:

$$\hat{B}_{I1} = Q_1^{j+1} - Q'' = 0 \tag{72}$$

in which Q'' is the computed flow at the last cross section of the supercritical reach and Q_1^{j+1} is the flow at the first cross section of the subcritical subreach. The downstream boundary for the subcritical subreach would be Eq. (46) if another supercritical subreach exists below the subcritical subreach or the appropriate condition described by Eqs. (40) - (46) if the subcritical subreach is the last subreach in the routing reach. The depth of flow at the first section of the subcritical subreach is determined by the downstream boundary condition and the Saint-Venant equations applied to the subcritical subreach. A hydraulic jump occurs between the last section of the supercritical subreach and the first section of subcritical subreach, although an equation for such is not directly used. To account for the possible movement of the hydraulic jump, the following procedure is utilized before advancing to the next time step: (1) the water elevation at the first section of the

subcritical subreach is extrapolated to several upstream cross sections near the downstream end of the supercritical subreach; (2) the sequent depths (water elevations) of the same sections in the supercritical reach are computed; and (3) the sequent elevations are compared with the extrapolated elevations, and the first section of the subcritical subreach is determined as that section nearest the intersection of two elevations.

CHANNEL NETWORKS

The implicit formulation of the Saint-Venant equations is well-suited from the standpoint of accuracy for simulating unsteady flows in a network of channels since the response of the system, as a whole, is determined within a certain convergence criteria for each time step. However, a network of channels presents complications in achieving computational efficiency when using the implicit formulation. Equations representing the conservation of mass and momentum at the confluence of two channels produce a Jacobian matrix in the Newton-Raphson method with elements which are not contained within the narrow band along the main-diagonal of the matrix. The column location of the elements within the Jacobian depends on the sequence numbers of the adjacent cross sections at the confluence. The generation of such "off-diagonal" elements produces a "sparse" matrix containing relatively few non-zero elements. Unless special matrix solution techniques are used for the sparse matrix, the computation time required to solve the matrix by conventional matrix solution techniques is so great as to make the implicit method infeasible. The same situation also occurs for the linearized implicit methods which must also solve a system of linear equations similar to the Jacobian. One of two algorithms can be selected in FLDWAV for an efficient computational treatment of channel networks.

The first, called the "relaxation" algorithm, is restricted to a dendritic (tree-type) network of channels in which the main channel has any number of tributary channels joining with it. Sometimes, dendritic systems with second-order tributaries (tributaries of tributaries) can be accommodated in the relaxation technique by reordering the dendritic system, i.e., selecting another branch of the system as the main channel. In the relaxation algorithm, no sparse matrix is generated; the Jacobian is always banded as it is for a single channel reach.

The second, called the "network" algorithm, can be used on almost any natural system of channels (dendritic systems having any order of tributaries; bifurcating channels such as those associated with islands, deltas, flow bypasses between parallel channels; and tributaries joining bifurcated channels). The network algorithm produces a sparse matrix which is solved by a special matrix technique which is described later. The relaxation algorithm is slightly more efficient than the network algorithm, but the former does not have the versatility of the latter.

Relaxation Algorithm. During a time step, the relaxation algorithm solves the Saint-Venant equations first for the main channel and then separately for each tributary of the first-order dendritic network. The tributary flow at each confluence with the main channel is treated as lateral flow (q) which is first estimated when solving Saint-Venant equations for the main channel. Each tributary flow depends on its upstream boundary condition,

lateral inflows along its reach, and the water surface elevation at the confluence (downstream boundary for the tributary) which is obtained during the simulation of the main channel. Due to the interdependence of the flows in the main channel and its tributaries, the following iterative or relaxation algorithm (Fread, 1973) is used:

$$q^* = \alpha q + (1 - \alpha) q^{**} \tag{73}$$

in which α is a weighting factor ($0 < \alpha \leq 1$), q is the computed tributary flow at each confluence, q** is the previous estimate of q, and q* is the new estimate of q. Convergence is attained when q is sufficiently close to q**, i.e., $|q - q^{**}| < \varepsilon_Q$. Usually, one or two iterations is sufficient; however, the weighting factor has an important influence on the algorithm's efficiency. Optimal values of α can reduce the iterations by as much as half. A priori selection of α is difficult since it varies with each dendritic system. Good first approximations for α are in the range, $0.6 \leq \alpha \leq 0.8$.

The acute angle (ω_t) that the tributary makes with the main channel is a specified parameter. This enables the inclusion of the momentum effect of the tributary inflow via the term ($-qv_x$) of Eq. (20) as used in the momentum equation, Eq. (2). The velocity of the tributary inflow is given by:

$$v_x = (Q/A)_N \cos \omega_t \tag{74}$$

in which N denotes the last cross section of the tributary.

Network Algorithm. The network algorithm is used when the channel network consists of any or all of the following: (1) second and higher-order tributaries; (2) bifurcations around islands with either zero, one, or two bypasses through the island; (3) dendritic branches joining any portion of the bifurcated branches; and (4) a dendritic network associated with river delta formations. The algorithm is based on the treatment of the channel junctions (confluences, bifurcations) as internal boundary conditions using the following three equations:

$$\hat{B}_{I1} = Q_i^{j+1} + Q_{i'}^{j+1} - Q_{i'+1}^{j+1} - \Delta s/\Delta t^j = 0 \tag{75}$$

$$\hat{B}_{I2} = 2g\left(h_i^{j+1} - h_{i'+1}^{j+1}\right) + \left(Q^2/A^2\right)_i^{j+1} - T\left(Q^2/A^2\right)_{i'+1}^{j+1} = 0 \tag{76}$$

$$\hat{B}_{I3} = 2g\left(h_{i'}^{j+1} - h_{i'+1}^{j+1}\right) + \left(Q^2/A^2\right)_{i'}^{j+1} - T\left(Q^2/A^2\right)_{i'+1}^{j+1} = 0 \tag{77}$$

where:
$$\frac{\Delta s}{\Delta t} = \Delta x_i/(6\Delta t^j)\,\tilde{B}\left(h_i^{j+1} + h_{i'}^{j+1} + h_{i'+1}^{j+1} - h_i^j - h_{i'}^j - h_{i'+1}^j\right) \tag{78}$$

$$i' = i + m + 1 \tag{79}$$

$$\tilde{B} = B_i^j + B_{i'+1}^j + B_{i'}^j \cos \omega_t \tag{80}$$

$$T = 1 + C_m + C_f \tag{81}$$

$$C_m = \left(0.1 + 0.83\, Q^j_{i'}/Q^j_{i'+1}\right)\left(\omega_t/90\right)^{\mu} \tag{82}$$

$$C_f = 2g\, \Delta x_i\, \bar{n}^2/\left[2.21\, \left(\bar{D}^{4/3}\right)^j\right] \tag{83}$$

in which $\bar{D}$ is the average depth in the junction, $\bar{n}$ is the Manning n for the junction, ω_t is the acute angle between the upstream reach and the branch, μ is an exponent taken as unity, and m is the total number of Δx reaches located upstream (downstream) along the branching channel. The parameters C_m and C_f are related to the head loss due to mixing (Lin and Soong, 1979) and friction effects, respectively. They can be specified as zero values in FLDWAV.

The rows in the matrix pertaining to the derivatives of Eqs. (75) - (77) are chosen so as to minimize the number of off-diagonal elements in the Jacobian and to minimize the creation of new off-diagonal elements during the elimination phase of the matrix solution. Also, the way in which the cross sections are assigned sequential numbers within the channel network is most important in effecting the desired minimization. The numbering scheme is as follows: numbers run consecutively in the downstream direction until a dendritic-type junction is reached; then the most upstream section of the dendritic branch is given the next consecutive number and the numbers increase in the downstream direction along this branch until another junction is reached; then the most upstream section of that dendritic branch is numbered and the numbers increase in the downstream direction along that branch until a new junction is reached; this is repeated until all sections have been numbered, including the first cross section of the branch of the very first dendritic-type junction; then the numbers continue to increase along the downstream branch of this junction. Bifurcations are numbered in a similar manner.

Computational efficiency is achieved by use of a specially developed matrix solution technique of the Gauss elimination type which operates on only non-zero elements in the matrix through use of a specified code number for each cross section in the network of channels. The specified code number is as follows: (1) regular cross section, (2) upstream boundary, (3) downstream boundary, (4) dendritic-type junction, (5) dendritic-type junction emanating from a bifurcated channel branch, (6) upstream junction of a bifurcation around an island, (7) downstream junction of a bifurcation around an island, (8) bifurcation-type junction emanating from another bifurcated channel and joining with a third bifurcated channel, and (9) bifurcation-type junction emanating from a bifurcated channel and joining into the other branch of the bifurcated channel.

Three subroutines in the FLDWAV program accomplish the special treatment of channel networks. The first determines the appropriate row and column numbers of the derivative elements in the Jacobian, the second evaluates the derivatives, and the third solves the matrix. The Jacobian is a 2N x 2N matrix. The number of operations (addition, subtraction, multiplication, division) required to solve the matrix is approximately (102 + 46J)N, where J is the total number of junctions. This is compared with (95N-48) operations for the relaxation algorithm, (38N-19) for a single channel using Eqs. (28) - (36), and $(16/3N^3+8N^2+14/3N)$ for a standard Gauss elimination method for solving a 2N x 2N matrix. Generally, the simulation of a channel network requires about one to two times as much computational effort as a single channel when each have N cross sections.

LEVEE EFFECTS

Flows which overtop a levee located along either side or both sides of a channel may be simulated in FLDWAV, since any number of Δx reaches may bypass flow via a broadcrested weir-flow equation to another channel which represents the floodplain (beyond the levee). If the system of channels including floodplain channels is treated by the relaxation technique, the floodplain channel may either directly connect back into the channel at some downstream location, or it may be disconnected as in the case of the floodplain within a ringed levee where the flow is ponded with no exit. The hydraulic connection may be either a natural confluence or a flap-gated gravity drainage pipe. The flow in the floodplain can affect the overtopping levee flows via a submergence correction factor K_{le} similar to that used at internal boundaries of dams. The flow may also pass from the channel to the floodplain through a time-dependent crevasse (breach) in the levee using a breach-flow equation similar to that used at internal boundaries of breached dams (Fread, 1980).

The overtopping and/or breach flow is routed through the floodplain which is considered to be a tributary of the channel along which the levee is located. The tributary (floodplain) channel must have a fictitious low-flow channel in which a small steady flow occurs at all times before the lateral inflow from the overtopped (breached) levee enters. The low flow which is specified via the upstream boundary condition for the tributary is necessary so that the Saint-Venant equations applied to the tributary can be continuously solved during the simulation; however, at the hydraulic connection with the channel, the fictitious low flow is not added to the channel flow nor is it included in the flow that ponds within a ringed levee. The floodplain may also be modeled as a reservoir using only Eq. (1) in which case no low flow condition need be considered.

Depending on the relative elevations in the channel and floodplain (tributary), the overtopping levee flow can reverse its direction and flow from the floodplain back into the channel. Each Δx_i reach for the channel has a corresponding Δx_m reach along the floodplain channel. Each Δx_i reach has a submergence correction factor (K_{le}), a broadcrested weir flow coefficient (C_{le}), and a mean elevation (h_{le}) of the top of the levee. The effect of the levee flow is achieved by considering it to be lateral inflow or outflow (q)

in Eqs. (1) and (2). When routing the flow in the channel, if the flow overtops the levee and enters the floodplain, it is considered to be bulk lateral outflow. When routing the flow in the floodplain, the levee overtopping flow is considered to be lateral inflow. In either case, the overtopping flow is computed as follows:

$$q_{le_i} = S_g \, C_{le_i} \, K_{le_i} \, (\hat{h} - h_{le_i})^{3/2} \quad \ldots \hat{h} > h_{le_i} \tag{84}$$

where:
$$S_g = (\hat{h} - \tilde{h})/|\hat{h} - \tilde{h}| \tag{85}$$

$$\hat{h} = \bar{h}_i \quad \ldots \bar{h}_i > h_{t_m} \tag{86}$$

$$\hat{h} = \bar{h}_{t_m} \quad \ldots \bar{h}_i < h_{t_m} \tag{87}$$

$$\tilde{h} = \bar{h}_{t_m} \quad \ldots \bar{h}_i > h_{t_m} \tag{88}$$

$$\tilde{h} = \bar{h}_i \quad \ldots \bar{h}_i < h_{t_m} \tag{89}$$

$$\bar{h}_i = 0.5 \, (h_i^{j+1} + h_{i+1}^{j+1}) \tag{90}$$

$$\bar{h}_{t_m} = 0.5 \, (h_{t_m}^{j+1} + h_{t_{m+1}}^{j+1}) \tag{91}$$

$$K_{le_i} = 1 \quad \ldots \gamma \leq 0.67 \tag{92}$$

$$K_{le_i} = 1. - 27.8 \, (\gamma - 0.67)^3 \quad \ldots \gamma > 0.67 \tag{93}$$

$$\gamma = (\tilde{h} - h_{le_i})/(\hat{h} - h_{le_i}) \tag{94}$$

in which S_g determines the appropriate sign (- for outflow, + for inflow), $\bar{h}_i$ is the average water elevation along the Δx_i reach, h_{t_m} is the average water elevation along the same Δx reach of the floodplain. Of course, the lateral flow may be zero when the water elevation in either channel does not overtop the levee or when the elevations are exactly the same, i.e.,

$$q_{le_i} = 0 \quad \ldots \hat{h} < h_{le_i}, \; \tilde{h} < h_{le_i} \tag{95}$$

$$q_{le_i} = 0 \quad \ldots \hat{h} = \tilde{h} \tag{96}$$

CROSS SECTIONS

That portion of the channel cross section in which flow occurs is termed active. In FLDWAV, the active flow cross sections may be of regular or irregular geometrical shape. Each cross section is specified as tabular values of channel width and elevation, which together constitute a piece-wise linear relationship. Experience has shown that, in almost all instances, the cross section may be sufficiently described with approximately eight or less sets of widths and associated elevations. The total cross-sectional area below each of the widths is initially computed within the model. During the solution of the unsteady flow equations, any areas or widths associated with a particular water surface elevation are linearly interpolated from the piece-wise linear relationships of width and elevation which were specified or the area-elevation sets initially generated within the model.

Cross-sections at gaging station locations are generally used as computational points in the x-t plane. Cross sections are also specified at points along the channel where significant cross-sectional changes occur or at points where major flows enter or exit. Typically, cross sections are spaced farther apart for large natural channels than for small channels, since the degree of variation in the cross-sectional characteristics is less for the larger channels. Spacing can range from a few hundred feet to a few miles.

CHANNEL FRICTION

The Manning n is used to describe the resistance of flow due to channel roughness caused by bed forms, bank vegetation, obstructions, bend effects, and eddy losses. The Manning n is defined for each Δx reach as a specified function of water elevation or discharge according to a tabular (piece-wise linear) relation between n and the independent variable (h or Q). Linear interpolation is used in FLDWAV to obtain n for values of h or Q intermediate to the tabular values.

LATERAL INFLOWS

FLDWAV incorporates small tributary inflows or overland flow via the lateral inflow term (q) in Eqs. (1) and (2). These are considered independent of flows occurring in the river to which they are added. They are specified as a time series of flows with constant or variable time intervals. They can be specified for any Δx reach along the river as the sum of all lateral inflows within the Δx reach. Outflows may be simulated by assigning a negative sign to the specified flows. Linear interpolation is used for flows at times other than the specified intervals.

MODEL CALIBRATION (AUTOMATIC)

Calibration is the process by which values of model parameters are adjusted until results of simulations correspond to measured (observed) flow conditions. A critical task in the calibration of dynamic wave models such as FLDWAV is the determination of the Manning n which often varies with discharge or stage, and with distance along the channel. Calibration may be a manual trial-and-error process; however, FLDWAV has an option to automatically determine the optimum Manning n which will minimize the difference between computed

and observed hydrographs via a highly efficient optimization technique (Fread and Smith, 1978). The technique can be applied to a single reach of channel or any dendritic system which can be simulated with the relaxation method. The Manning n or conveyance factor (K_c) may be constant or have a piece-wise linear variation with either discharge or water elevation for each reach of the channel bounded by gaging stations from which observed water elevation hydrographs are available.

In the automatic calibration technique optimum Manning n values are sequentially determined for each reach bounded by gaging stations, commencing with the most upstream reach and progressing reach-by-reach in the downstream direction. Dendritic river systems are decomposed into a series of single reaches connected by appropriate external boundary conditions. Tributaries are calibrated before the main-stem channel and their flows are added to the main stem as lateral inflows. An observed discharge hydrograph is specified at the upstream boundary of each channel, while an observed water elevation hydrograph at the downstream gaging station of each reach is used as the downstream boundary condition. The computed water elevation hydrograph at the upstream boundary is tested against the observed hydrograph at that point. Statistics of bias (Φ_j) and root-mean-square (RMS) error are computed for j=1,2,3, ... J ranges of discharge or water elevation so that the Manning n or K_c can be calibrated as a function of discharge or stage. For each range of discharge, an improved estimate of the optimum Manning n (n_j^{k+1}) is obtained via a modified Newton-Raphson iterative method, i.e.,

$$n_j^{k+1} = n_j^k - \frac{\Phi_j^k \left(n_j^k - n_j^{k-1}\right)}{\left(\Phi_j^k - \Phi_j^{k-1}\right)} \qquad \ldots k > 2; j = 1,2,\ldots J \qquad (97)$$

in which the k superscript denotes the number of iterations and Φ_j is the bias for the j^{th} range. Eq. (97) can be applied only for the second and successive iterations; therefore, the first iteration is made using the following estimator:

$$n_j^{k+1} = n_j^k \left(1.0 - 0.01\ \Phi_j^k / |\Phi_j^k|\right) \qquad \ldots k = 1; j = 1,2,\ldots J \qquad (98)$$

in which a small percentage change in the Manning n is made in the correct direction as determined by the term $(-\Phi_j^k / |\Phi_j^k|)$. The convergence properties of Eq. (97) are quadratic with convergence usually obtained within three to four iterations. Improved Manning n values obtained via Eq. (97) are used and the cycle repeated until a minimum RMS error for the reach is found. Then, the discharges computed at the downstream boundary using the optimum Manning n are stored internally and specified as the upstream boundary condition for the next downstream reach.

Computational requirements for the calibration technique are less than twice that required for an application of FLDWAV to the same channel without the calibration option utilized.

COMPUTATIONAL PROPERTIES

The computational properties of the 4-point implicit solution of the Saint-Venant equations was reported by Fread (1974). Numerical Stability was found to depend primarily on the θ weighting factor of Eqs. (6)-(8). A generalized stability relationship was found for the 4-point implicit method applied to the following simplified forms of Eqs. (1) and (2) including linear friction:

$$\frac{\partial h}{\partial t} + D_o \frac{\partial V}{\partial x} = 0 \tag{99}$$

$$\frac{\partial V}{\partial t} + g\frac{\partial h}{\partial x} + kV = 0 \tag{100}$$

in which $k = \dfrac{2gV_o}{C^2 D_o}$, (101)

h is the water surface elevation, C is the Chezy friction coefficient, and D_o and V_o are initial values of hydraulic depth and velocity, respectively. An expression for stability (in the sense of the von Neumann conjecture that linear operators with variable coefficients are stable if all their localized operators in which the coefficients are taken constant are stable) is given by the following expression:

$$|\lambda| = \left[\frac{1 + (2\theta - 2)^2 a + (\theta - 1)b}{1 + 4\theta^2 a + \theta b}\right]^{1/2} \tag{102}$$

in which $a = gD_o(\Delta t/\Delta x)^2 \tan^2(\pi\Delta x/L)$; $b = k\Delta t$; and L = wavelength = wave celerity x duration. If $|\lambda| < 1$, independent of the values of Δx and Δt, the errors due to truncation and round-off will not grow with time, and the difference equations are unconditionally linearly stable. This is the case when $0.5 \leq \theta \leq 1$, although only weakly stable (i.e., $|\lambda| = 1$) when $\theta = 0.5$ and k approaches zero. Accuracy of the weighted 4-pt. scheme depends on the selection of Δt , i.e.,

$$\Delta t \leq 0.11\, c\, Z\, T_p/\sqrt{D_o} \tag{103}$$

where: $$Z = \left[\frac{1 - \varepsilon^2}{4\theta^2\,\varepsilon^2 - (2\theta - 2)^2}\right]^{1/2} \tag{104}$$

in which T_p is the time of rise of the flood wave in hours, c is the wave celerity in ft/sec, ε is the permissible error ratio, $0.90 \leq \varepsilon \leq 0.99$, and Δt is the time step in hours.

The required computational time using an IBM 360/195 mainframe computer varies from about 0.001 to 0.005 sec per Δx per Δt depending on the complexity of the system of channels and the extent of nonlinearity of the water wave and channel characteristics.

SUMMARY AND CONCLUSIONS

Unsteady flow simulation models such as the National Weather Service's DWOPER and its recent enhancement FLDWAV have been developed for application to river-reservoir-estuarial systems. However, they have the potential for both real-time simulation and/or operational planning and design of irrigation systems. The mathematical and hydraulic aspects of FLDWAV have been described herein. The basis for the model is the one-dimensional equations of unsteady flow (Saint-Venant equations) which are two nonlinear partial differential equations. These are solved by an implicit finite difference solution technique using a weighted 4-point scheme. The resulting finite difference equations are nonlinear and are solved simultaneously for all points within the system of channels. An iterative technique (Newton-Raphson) along with special matrix solution techniques based on Gaussian elimination enable efficient solutions to be obtained. Special flow and level controls within the system of channels can be simulated via their inclusion as internal boundary conditions. The system of channels can range in complexity from a single channel to a network of channels. Levee overtopping/failure and landslide blockages could be simulated for operational planning purposes.

REFERENCES

Amein, M. and Fang, C.S. (1970). 'Implicit flood routing in natural channels', J. Hydr. Div., ASCE, Vol. 96, No. HY12, pp. 2481-2500.

Fread, D.L. (1971). 'Discussion of implicit flood routing in natural channels by M. Amein and C. S. Fang', J. Hydr. Div., ASCE, Vol. 97, No. HY7, pp. 1156-1159.

Fread, D.L. (1973). 'Technique for implicit dynamic routing in rivers with tributaries', Water Resources Research, Vol. 9, No. 4, pp. 918-926.

Fread, D.L. (1974). Numerical Properties of Implicit Four-point Finite Difference Equations of Unsteady Flow, NOAA Tech. Memo NWS HYDRO-18, U.S. Department of Commerce, National Weather Service, Silver Spring, Maryland.

Fread, D.L. (1978). 'NWS operational dynamic wave model', in Verification of Mathematical and Physical Models, Proc. of 26th Annual Hydr. Div. Specialty Conf., ASCE, College Park, Maryland, pp. 455-464.

Fread, D.L. (1980). 'Capabilities of NWS model to forecast flash floods caused by dam failures', in Proc., 2nd Conf. on Flash Floods, Atlanta, Georgia, American Met. Soc., pp. 171-178.

Fread, D.L. and Smith, G.F. (1978). 'Calibration technique for 1-D unsteady flow models', J. Hydr. Div., ASCE, Vol. 104, No. HY7, pp. 1027-1044.

Lin, J.O. and Soong, H.K. (1979). 'Junction losses in open channel flows', Water Resources Research, Vol. 15, No. 2, pp. 414-418.

Preissmann, A. (1961). 'Propagation of translatory waves in channels and rivers', in Proc., First Congress of French Assoc. for Computation, Grenoble, France, pp. 433-442.

Saint-Venant, B. De. (1871). 'Theory of unsteady water flow, with application to river floods and to propagation of tides in river channels', Computes rendus, Vol. 73, Acad. Sci., Paris, pp. 148-154, 237-240. (Translated into English by U.S. Corps of Engineers, No. 49-g, Waterways Experiment Station, Vicksburg, Missippi, 1949.)